Inverse dielectric response function for copper oxide superconductors

A. C. Sharma and Ina Kulshrestha
School of Studies in Physics, Jiwaji University, Gwalior-474011, India
(Received 9 April 1992)

We use a layered-electron-gas model to calculate the inverse electronic dielectric response functions for the normal state of copper oxide superconductors with one and two copper oxide layers per unit cell. Our calculation demonstrates that the low-energy electronic collective-excitation spectrum consists of both acoustic and optic plasmons. The acoustic plasmon modes are found to be well behaved only for certain restricted values of the wave vector and damping parameter. Our computed optical inverse dielectric response function exhibits one peak in the low-energy region and varies as $\beta\omega^2$ for $0 \leq \omega \leq \omega_p$. Here β is a material-dependent parameter and ω_p is the position of the peak that corresponds to the intraband optic plasmon mode. Our calculated optical dielectric response functions show excellent agreement with the experimental results of Bozovic for $0 \leq \omega \leq \omega_p$.

I. INTRODUCTION

The plasmons in copper oxide ceramics have been the subject of immense interest, ever since the discovery of high-temperature superconductivity in these materials.[1-6] There have been several experimental and theoretical studies on the plasmons and the electron-energy-loss function for the copper oxide ceramics. The reason for this interest is twofold: First, many proposed theoretical mechanisms of the high-temperature superconductivity are based on a plasmon-mediated electron-electron interaction potential.[7-12] (The kind of plasmon modes proposed to give rise to an attractive interaction potential varies from calculation to calculation, however.) Second, the plasma frequency ω_p is one of the key parameters required to characterize the normal state of a superconductor. In order to elucidate a plasmon-based mechanism of high-T_c superconductivity, one requires complete knowledge of the low-energy electronic excitations, which can be inferred from the inverse dielectric response function (IDRF) of the system. Moreover, many-body theories of several important properties, such as light scattering, electron energy loss, reflection and absorption of light, conductivity, etc., can be built around the IDRF. In view of this, we use in this paper, a layered-electron-gas (LEG) model to perform a calculation of the IDRF for the normal state of copper oxide ceramics.

The IDRF, together with the real and imaginary parts of dielectric response function, has recently been measured by several workers[1,3,4] for the normal state of $La_{2-x}Sr_xCuO_4$, $YBa_2Cu_3O_7$, and $Tl_2Ba_2Ca_2Cu_3O_{10}$ superconductors. Bozovic[1] measured the optical IDRF of $YBa_2Cu_3O_7$, $Bi_2Sr_2CaCu_2O_8$, and $Tl_2Ba_2Ca_2Cu_3O_{10}$. He found (i) that the IDRF varies as βw^2 for $0 \leq \omega \leq \omega_p$, where β is a material-dependent parameter, (ii) that there is only one broad peak in the IDRF in the low-energy region, and (iii) that the plasmon spectrum consists of both optic and acoustic plasmon modes. The measured behavior is certainly not Drude-like. Bozovic suggested that his measured behavior of IDRF may be compatible with the LEG model. The low-energy collective excitations have also been measured by Nücker *et al.* for $Ba_2Sr_2CaCu_2O_8$, using electron-energy-loss spectroscopy (EELS). They observed that the measured plasmon mode is a well-behaved optic plasmon mode for small values of q, which is the a-b-plane component of wave vector. However, for higher q values, the observed mode is strongly damped, showing that it is in a region of intraband and interband excitations. The peak height of measured IDRF is found to decrease with increasing q.

This paper deals with the calculation of IDRF for the normal state of ceramics, such as $La_{2-x}Sr_xCuO_4$, with one Cu-O layer per unit cell and ceramics such as $Ba_2Sr_2CaCu_2O_8$, with two Cu-O layers per unit cell. The main assumptions of our calculation are as follows: the single crystal of a copper oxide ceramic can be viewed as an infinite array of Cu-O layers separated from one another by a block of nonconducting layers. A Cu-O layer consists of free charge carriers and the bound electrons; the latter are also found in the nonconducting layers. The system can therefore be modeled to be an array of two-dimensional sheets of charge carriers (2DSCC), which are embedded in a layered polarizable dielectric host medium with dielectric constant $\epsilon_B(\omega)$. The distance between any two consecutive Cu-O layers of ceramics, such as $La_{2-x}Sr_xCuO_4$ is the same and hence, a model unit cell can be constructed by joining two consecutive 2DSCC. For ceramics like $Ba_2Sr_2CaCu_2O_8$, three consecutive Cu-O layers are periodically repeated and a model unit cell can be made by joining any three consecutive 2DSCC. The length of the unit cell along the c axis is taken to be d for both cases. The distance between the bottom and the middle 2DSCC for materials like $Ba_2Sr_2CaCu_2O_8$ is taken to be d_1.

Our calculation shows the following: (i) the LEG model does yield a ω^2 dependence of the IDRF for $0 \leq \omega \leq \omega_p$ for normal-incidence light, (ii) the peak height of the IDRF decreases with increasing q. We have to, however, take a linear ω dependence for the damping parameter γ in our calculation. We also find that plasmon spectrum consists of both optic and acoustic plasmon modes. However, the acoustic plasmon modes are very sensitive

to changes in q and γ; they cease to exist for higher values of q and γ. The remainder of this paper is organized as follows: the details of our calculation are given in Sec. II. We present, in Sec. III, a discussion of our results. Our work is then summarized in Sec. IV.

II. CALCULATIONAL DETAILS

Our model system consists of conduction charge carriers confined in 2D sheets along a-b planes and of bound electrons which are associated with the host medium. The 2D charge carriers give rise to low-energy intraband plasmons, while the bound electrons can yield interband plasmons. The effective interaction potential for model system can be given as[13,14]

$$V_{ij}(q,\omega,q_z)=\sum_{j'=0}^{1}\epsilon_{ij'}^{-1}(q,\omega,q_z)V_{j'j}^{0}(q,\omega,q_z)\ , \tag{1}$$

where $\epsilon_{ij}^{-1}(q,\omega,q_z)$ is the inverse of $\epsilon_{ij}(q,\omega,q_z)$. The $\epsilon_{ij}(q,\omega,q_z)$ and $V_{ij}^{0}(q,\omega,q_z)$ are given by

$$\epsilon_{ij}(q,\omega,q_z)=\epsilon_B(\omega)\delta_{ij}-V_{ij}^{0}(q,\omega,q_z)\pi(q,\omega)\ , \tag{2}$$

$$V_{ij}^{0}(q,q_z)=\frac{2\pi e^2}{q}\left[\frac{\exp(-q|R_{ij}|l)+\exp(iq_zd)}{\exp(iq_zd)-\exp(-qd)}+\frac{\exp(-q|R_{ij}|l)-\exp(-qd)}{\exp(iq_zd)-\exp(-qd)}\right]\ , \tag{3}$$

with

$$\epsilon_B(\omega)=1+\frac{E_p^2}{E_g^2-(\omega+i\alpha)^2}\ ,$$

and (4)

$$V_{ij}^{0}(q,q_z)\equiv V_{ji}^{0}(q,-q_z)\equiv V_{ji}^{0*}(q,q_z)\ .$$

In Eqs. (1)–(4) i, j, and j' represent the indices of 2DSCC in a unit cell. The q_z is the component of wave vector along the c axis. R_{ij} is the distance between the ith and jth 2DSCC in a unit cell. E_p and E_g are, respectively the plasma energy and energy-band gap for interband transitions. Equation (1) yields the effective intralayer interaction potential for $i=j$, while for $i\neq j$ it gives the effective interlayer interaction potential. For systems with one 2DSCC per unit cell, i, j, and j' can take on only one single value of either 0 or 1, while for systems with two 2DSCC per unit cell, i, j, and j' can be assigned two values, 0 and 1. In the former case, Eq. (1) gives only the diagonal terms V_{00} and V_{11}, which are identical and can be given

$$V_1(q,q_z,\omega)=V_{00}^{0}/[\epsilon_B(\omega)+P(q,\omega)S(q,\omega)]\ , \tag{5}$$

where V_{00}^{0} can be simplified to $(2\pi e^2/q)S(q,q_z)$, with

$$S(q,q_z)=\frac{\sinh(qd)}{\cosh(qd)-\cos(q_zd)}\ . \tag{6}$$

The $P(q,\omega)$ is the dynamical susceptibility defined as

$$P(q,\omega)=-\frac{2\pi e^2}{q}\pi(q,\omega)\ . \tag{7}$$

Equation (1) yields two diagonal terms (V_{00} and V_{11}) and two off-diagonal terms (V_{01} and V_{10}) for systems with two 2DSCC per unit cell. The diagonal terms, which are identical, give rise to an effective intralayer potential $V_2(q,q_z,\omega)$, while the off-diagonal terms describe the interlayer interaction potentials $V_3(q,q_z,\omega)$ and $V_4(q,q_z,\omega)$. We can then write

$$V_2(q,q_z,\omega)=V_{00}^{0}[\epsilon_B(\omega)+P(q,\omega)f(q)]/\epsilon(q,q_z,\omega)\ , \tag{8}$$

$$V_3(q,q_z,\omega)=V_{01}^{0}\epsilon_B(\omega)/\epsilon(q,q_z,\omega)\ , \tag{9a}$$

$$V_4(q,q_z,\omega)=V_{10}^{0}\epsilon_B(\omega)/\epsilon_B(q,q_z,\omega)\ , \tag{9b}$$

with

$$\epsilon(q,q_z,\omega)=\epsilon_B^2(\omega)+[2\epsilon_B(\omega)+P(q,\omega)f(q)]P(q,\omega)S(q,q_z)\ , \tag{10}$$

$$f(q)=[\cosh(qd)-\cosh(qd')]/\sinh(qd)\ . \tag{11}$$

Here, $d'=2d_1-d$. The model IDRF for materials such as $La_{2-x}Sr_xCuO_4$ is given by V_1/V_{00}^{0}. For materials such as $Ba_2Sr_2CaCu_2O_4$, V_{ij} forms a 2×2 matrix. The eigenvalues of the matrix give rise to the two effective IDRF of our model system:

$$T_{\pm}(q,\omega,q_z)=\frac{V_2(q,\omega,q_z)}{V_0^{00}(q,q_z)}\pm\frac{\epsilon_B(\omega)[V_{01}^{0}(q,q_z)V_{10}^{0}(q,q_z)]^{1/2}}{V_{00}^{0}(q,q_z)\epsilon(q,\omega,q_z)}\ . \tag{12}$$

$T_{\pm}$ corresponds to the in-phase and out-of-phase oscillations of the two 2DSCC of a unit cell. The IDRF for single 2DSCC in materials with one or two 2DSCC per unit cell can be evaluated by dividing the q_z average of $V_1(q,q_z,\omega)$ and $V_{00}^{0}T_{\pm}(q,q_z,\omega)$ by $2\pi e^2/q$, respectively. The average of $V_{00}^{0}T_{\pm}$ does not significantly differ from that of $V_2(q,\omega,q_z)$. The q_z averages of $V_1(q,q_z,\omega)$ and $V_2(q,q_z,\omega)$ are given as

$$V_1(q,\omega)=\frac{2\pi e^2}{q}C_{\pm}/[G^2(q,\omega)-\epsilon_B^2(\omega)\mathrm{csch}^2(qd)]^{1/2}\ , \tag{13}$$

$$V_2(q,\omega)=\frac{2\pi e^2}{q}D_{\pm}[\epsilon_B(\omega)+P(q,\omega)f(q)]/[H^2(q,\omega)-\epsilon_B^4(\omega)\mathrm{csch}^2(qd)]^{1/2}\ , \tag{14}$$

with

$$G(q,\omega)=\epsilon_B(\omega)\coth(qd)+P(q,\omega)\ , \tag{15}$$

$$H(q,\omega)=\epsilon_B^2(\omega)\coth(qd) +P(q,\omega)[2\epsilon_B(\omega)+P(q,\omega)f(q)]\ . \tag{16}$$

Here, $C_\pm$ and $D_\pm$ denote the signs of the real parts of $G(q,\omega)$ and $H(q,\omega)$, respectively.

A realistic calculation of $P(q,\omega)$ for single 2DSCC depends on several aspects of the behavior of charge carriers. Marginal-Fermi-liquid[15] and nested-Fermi-liquid[16] theories have been proposed for calculations of an appropriate $P(q,\omega)$ for the copper oxide ceramics. Random-phase-approximation (RPA) forms of $P(q,\omega)$ have also been used to describe the plasmons and electron-energy-loss function of the copper oxide ceramics.[5,6] As we too aim to evaluate the plasmon dispersion relation and IDRF, we use the RPA $P(q,\omega)$ in Eqs. (5)–(13). However, we also introduce a linear ω dependence in γ in order to take into account strong correlation effects, in an *ad hoc* manner.[16] The collective excitation modes are usually well defined for small q and ω, and so a realistic form of the RPA $P(q,\omega)$ for a 2DSCC can be taken as

$$P(q,\omega)=\frac{qe^2k_F^2/m^*}{q^2v_F^2/2-\omega^2(1+i\delta)^2}\ , \tag{17}$$

where k_F and v_F are the Fermi wave vector and Fermi velocity, respectively. m^* is the effective mass of a charge carrier.

III. RESULTS AND DISCUSSIONS

The plasmons in materials such as $La_{2-x}Sr_xCuO_4$ are given by the zeros of V_{00}^0/V_1, while that of materials such as $Ba_2Sr_2CaCu_2O_8$ are given by the poles of $T_\pm(q,q_z,\omega)$. The zeros of V_{00}^0/V_1 give rise to a full band of in-plane plasmon modes. The lower and upper edge of the band occur at $q_zd=\pi$ and at $q_zd=0$, respectively. The band consists of acoustic and optic plasmons. This can be more explicitly seen from Eq. (13). The poles of Eq. (13) yield two plasmon modes; the lower one behaves as $\omega_{p-}\sim\omega_1qd/2$, while the upper mode ω_{p+} tends to ω_1 as $q\to0$, where $\omega_1=2e^2k_F^2/m^*d$. On the other hand, the poles of $T_\pm(q,q_z,\omega)$ give rise to two bands of in-plane plasmon modes. The upper band is very much similar to that obtained from the zeros of V_{00}^0/V_1. This band again consists of acoustic and optic plasmons. However, the lower band consists of only acoustic plasmons. The poles of the Eq. (14) yield four plasmon modes, three of which are of acoustic nature, while the fourth is an optic plasmon mode. As $q\to0$, they are approximately $\omega_{p1}\sim(2/3)^{1/2}\omega_1qd$, $\omega_{p2}\sim(1/6)^{1/2}\omega_1qd$, $\omega_{p3}\sim(1/3)\omega_1qd$, and $\omega_{p4}\sim(2)^{1/2}\omega_1$. The acoustic plasmon modes are found to be well behaved only for small q and δ values; for higher values of q and δ, these modes cease to exist. For oxide ceramics, δ is reasonably high (because of low mobility) and acoustic plasmons are severely damped and therefore have not been observed in light-scattering and EELS experiments. The optic plasmon modes, on the other hand, are well behaved for reasonably high values of q and δ. The optic plasmons have been observed in both light-scattering as well EELS experiments. Nücker *et al.* has measured the electron-energy-loss function of $Ba_2Sr_2CaCu_2O_8$ for various q values, using EELS. They observed only one peak in the loss function in the low-energy range; this peak corresponds to the intraband optic plasmon mode. They also found that the height of peak decreases with increasing q.

We computed $T_\pm(q,\omega,q_z)$ as a function of ω at different q and δ values for $q_z\to0$. For computation, we used $m^*=1.4\ m_e$, $n=5.2\times10^{21}$ cm^{-3}, $d=30.8$ Å, $E_p=8.4$ eV, $E_g=5.3$ eV, and $\alpha=1.2\omega$ eV. We found that $T_\pm(q,\omega,q_z)$ exhibits two peaks for $0\le\delta\le0.2$ and $0\le q\le0.5$ Å^{-1}. For $\delta\ge0.2$ there is only one peak at all q values. We found that our calculated peak positions of $T_\pm$ show excellent agreement with those of measured energy-loss function at all q values, for $\delta=0.3$, as it can be seen from the Fig. 1. In Fig. 2, we plot our calculated peak height of $T_\pm(q,\omega,q_z)$ as a function q. The figure demonstrates that the peak height decreases with the increase of q. This is in accordance with the experimental observations of Nücker *et al.*[4]

In order to compare our calculation with the experimental results of Bozovic[1] on optical IDRF, we computed the q- and q_z-averaged imaginary part of

$$T_\pm(q,\omega,q_z)V_{00}^0(q,q_z)\ .$$

Our q- and q_z-averaged imaginary part of

$$T_\pm(q,\omega,q_z)V_{00}^0(q,q_z)$$

divided by $2\pi e^2d$ corresponds to the optical IDRF for

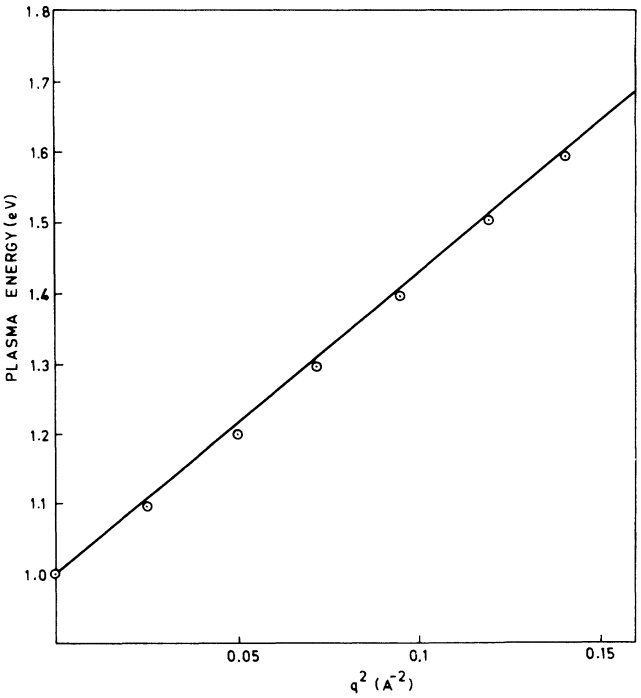

FIG. 1. Plasmon energy as a function of q^2. Our calculation (solid line). Dotted open circles are experimental points from Ref. 4.

normal incidence of light, which has been the case in Bozovic's experiments. We used above mentioned values of m^*, n, d, E_p, E_g, and α. The δ is taken to be 0.16. Our computed optical IDRF along with the experimental results of Bozovic is plotted in Fig. 3, for $Ba_2Sr_2CaCu_2O_8$. As we can see from the figure, our calculated optical IDRF shows only one peak in the low-energy range and varies as $\beta\omega^2$ for $0 \leq \omega \leq \omega_p$. The ω_p is the position of the peak corresponding to ω_{p4}. Our theoretical results are also seen to be in excellent agreement with the experimental data for $0 \leq \omega \leq \omega_p$. The agreement between our calculation and the experimental results is, however, not very good for $\omega \geq \omega_p$. The reason may be that our model calculation does not properly incorporate interband transitions, which contribute significantly for $\omega \geq \omega_p$. We also calculated the Drude IDRF, using a linear ω-dependent damping parameter. The best possible agreement between the Drude IDRF and the experimental data can be obtained with the use of $\omega_p = 15$ eV, $\alpha \equiv \gamma = 0.62\omega$ eV, $E_p = 10$ eV, and $E_g = 7$ eV. The Drude formula also gives $\beta\omega^2$ of the IDRF for small-ω values. However, the Drude formula does not reproduce any part of the experimental curve, for any possible choice of values of the parameters. In passing, we would like to mention that Virosztek and Ruvalds[17] used a ω dependence of m^*, together with a linear ω dependence of γ, in the Drude formula, in order to obtain a good agreement between their calculation and the experimental results. However, the value of γ used in the Drude formula seems to be too high a value of damping constant for using the Fermi-liquid quasiparticle hypothesis. On the other hand, the value of γ used in our calculation is reasonably compatible with the quasiparticle hypothesis. We note here that the Drude formula does not incorporate the acoustic plasmon modes. We therefore can conclude that the $\beta\omega^2$ of our calculated IDRF comes partly from the linear ω dependence of γ and partly from the acoustic plasmon modes. The ω^2 dependence of the IDRF due to acoustic plasmon modes has also been pointed out by Bozovic.[1] During our computation, we notice that β is very sensitive to the changes in m^*, δ, E_p, and E_g. From our calculation, we estimate $\beta = 0.31$ for $Ba_2Sr_2CaCu_2O_8$.

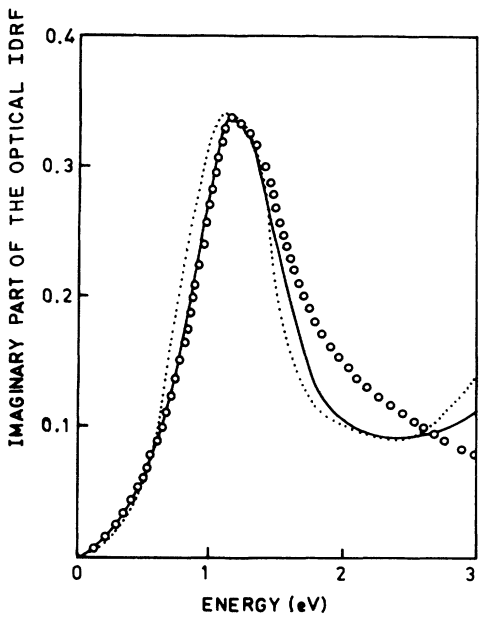

FIG. 3. The imaginary part of optical inverse dielectric response function plotted as function of ω for $Ba_2Sr_2CaCu_2O_8$. The open-circle curve shows experimental results from Ref. 1. The solid curve is from our calculation, and the dotted curve is from the Drude model.

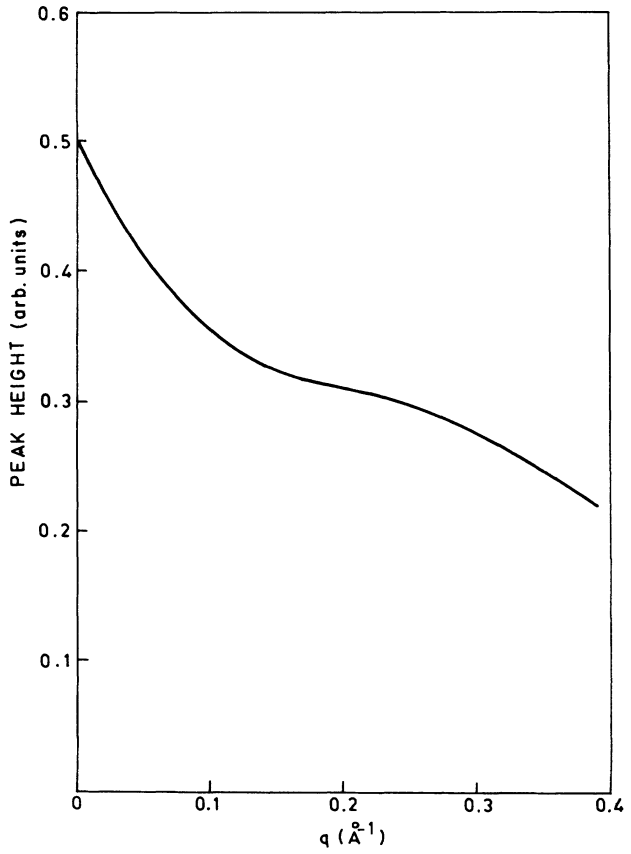

FIG. 2. The peak height of inverse dielectric response function plotted as a function of q.

In Fig. 4, we plotted our calculated optical IDRF along with the experimental results of Bozovic[1] for $YBa_2Cu_3O_7$. We used $m^* = 1.25m_e$, $d = 11.7$ Å, $n = 7 \times 10^{21}$ cm^{-3}, $E_p = 6.7$ eV, $E_g = 5.1$ eV, $\alpha = 0.9\omega$ eV, and $\delta = 0.18$, for our computation. Our calculated optical IDRF for $YBa_2Cu_3O_7$ also varies as $\beta\omega^2$ and shows an excellent agreement with the experimental results of Bozovic for $0 \leq \omega \leq \omega_p$, as it can be seen from the figure. We estimate $\beta = 0.21$ for $YBa_2Cu_3O_7$ from our calculation.

Our computed optical IDRF for $La_{2-x}Sr_xCuO_4$ is plotted in Fig. 5. For our computation, we used $m^* = m_e$, $d = 13.25$ Å, $\delta = 0.25$, $\alpha = 0.9\omega$ eV, $E_p = 8$ eV, $\delta = 0.21$, $E_g = 6.2$ eV, and $n = 5 \times 10^{21}$ cm^{-3}. As it can be seen from the figure, our calculated optical IDRF

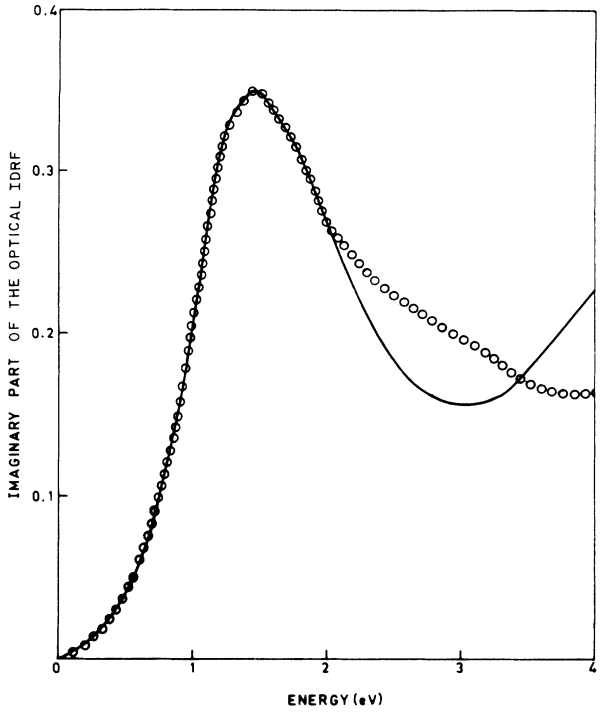

FIG. 4. Plot of the imaginary part of optical inverse dielectric response function for $YBa_2Cu_3O_7$. The (open-circle) curve shows experimental results from Ref. 1. The solid curve is from our calculation.

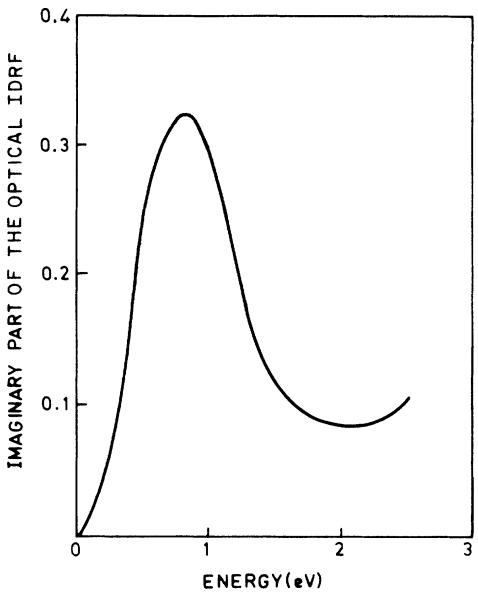

FIG. 5. The imaginary part of our calculated optical inverse dielectric response function for $La_{2-x}Sr_xCuO_4$.

varies as $\beta\omega^2$ for $La_{2-x}Sr_xCuO_4$ too, for $0 \leq \omega \leq \omega_p$. We estimate $\beta = 0.87$ for $La_{2-x}Sr_xCuO_4$ from our calculation.

IV. CONCLUSIONS

We calculated the IDRF for the copper oxide ceramics with either one or two Cu-O layers per unit cell. We find that the low-energy plasmon spectrum consists of both acoustic and optic plasmon modes. A 2DSCC for ceramic with a one Cu-O layer per unit supports one acoustic and one optic plasmon mode. On the other hand, a 2DSCC for ceramics with two Cu-O layers per unit cell supports three acoustic and optic plasmon modes. However, the acoustic plasmon modes are severely damped and hence may not be observed in EELS and light-scattering experiments. Our calculation shows that the peak height of the optic plasmon mode decreases with increasing q, which is in agreement with the experimental observations of Nücker *et al.* Our calculated optical IDRF shows only one peak and varies as $\beta\omega^2$ for $0 \leq \omega \leq \omega_p$ in the low-energy range. Also, our IDRF shows an excellent agreement with the experimental results of Bozovic,[1] for $0 \leq \omega \leq \omega_p$, for $Ba_2Sr_2CaCu_2O_8$ and $YBa_2Cu_3O_7$. The value of β depends on the various parameters used in our calculations.

ACKNOWLEDGMENTS

Part of the work has been completed during the visit by one of us (A.C.S.) to the Indian Institute of Science, Bangalore. A.C.S. is indebted to Professor T.V. Ramakrishnan for many valuable suggestions on the problem and for a critical reading of this manuscript. The work is supported by the Council of Scientific and Industrial Research, New Delhi.

[1] I. Bozovic, Phys. Rev. B **42**, 1969 (1990), and references therein.
[2] S. Tajima, T. Nakahashi, S. Uchida, and S. Tanaka, Physica C **156**, 90 (1988).
[3] I. Bozovic, J. H. Kim, J. S. Harris, Jr., and W. Y. Lee, Phys. Rev. B **43**, 1169 (1991).
[4] N. Nücker, H. Romberg, S. Nakai, B. Scheerer, J. Fink, Y. F. Yan, and Z. X. Zhao, Phys. Rev. B **39**, 12 379 (1989).
[5] G. D. Mahan and J. W. Wu, Phys. Rev. B **39**, 265 (1989).
[6] S. F. Tsay, S. Y. Wang, and T. J. Watson Yang, Phys. Rev. B **43**, 13 080 (1991), and references therein.
[7] S. M. Cui and C. H. Tsai Phys. Rev. B **44**, 12 500 (1991).
[8] J. Ruvalds, Phys. Rev. B **35**, 8869 (1987).
[9] A. C. Sharma, Solid State Commun. **70**, 1171 (1989).
[10] A. Griffin, Phys. Rev. B **37**, 5843 (1988).
[11] V. Z. Kresin, Phys. Rev. B **35**, 8716 (1987); V. Z. Kresin and H. Morawitz, *ibid.* **37**, 7854 (1988).
[12] J. Askenazi, C. G. Kuper and R. Tyk, Physica B **148**, 366 (1987).
[13] A. C. Sharma, Mod. Phys. Lett. B **5**, 444 (1991).
[14] S. S. Jha, Pramana **29**, L615 (1987).
[15] C. M. Verma, P. B. Littlewood, S. Schmitt-Rink, E. Abrahams, and A. E. Ruckenstein, Phys. Rev. Lett. **63**, 1996 (1989).
[16] A. Virosztek and J. Ruvalds, Phys. Rev. B **42**, 4064 (1990).
[17] A. Virosztek and J. Ruvalds, Phys. Rev. B **45**, 347 (1992).